ORGANIC CHEMISTRY FRONTIERS

RESEARCH ARTICLE

View Article Online
View Journal | View Issue



Cite this: *Org. Chem. Front.*, 2021, **8**, 3244

# Clover leaf-shaped supramolecules assembled using a predesigned metallo-organic ligand†

Qixia Bai,‡[a] Tun Wu,‡[a] Zhe Zhang,*[a,c] Lianghuan Xu,[a] Zhengbin Tang,[a] Yuming Guan,[a] Ting-Zheng Xie,[a] Mingzhao Chen,[a] Peiyang Su,[a] Heng Wang,[b] Pingshan Wang *[a] and Xiaopeng Li *[b]

Received 28th February 2021,
Accepted 1st April 2021

DOI: 10.1039/d1qo00336d

rsc.li/frontiers-organic

Inspired by the clover plant in nature, clover leaf-shaped supramolecular structures with three hexagons fused to create a triangular core were designed and self-assembled using a combination of Ru–Zn, Ru–Co, Ru–Mn or Ru–Ni metal ions. These results lay the foundation for further applications of heterometallic multinuclear metallo-supramolecules.



An important subfield of supramolecular chemistry, coordination-driven self-assembly has emerged in many synthetic systems that have dynamic characteristics over the past few decades.[1,2] These metallo-supramolecular structures, that have increasing complexity and diversity, play an increasingly significant role in catalysis,[3] sensing,[4] drug delivery and release,[5] gas storage,[6] and smart materials[7] due to their specific sizes and shapes. Of the diverse library of organic building blocks that exist, 2,2′:6′,2″-terpyridine (tpy) has been extensively used as a tridentate motif because of its excellent complexation ability toward different metal ions.[8] In addition to the common one-step self-assembly methodology that utilizes organic ligands and metal ions, the kinetically inert <tpy-$Ru^{2+}$-tpy> connectivity allows for an alternative step-wise self-assembly approach for constructing supramolecular structures with increased complexity.[9] Usually, a stable Ru(II)-organic ligand is synthesized and subsequently self-assembles with other metal ions with weak coordination, such as Zn(II), Cd(II) and Fe(II), to form heterometallic metallo-supramolecules.[10] However, the lack of other suitable metal ions has created great obstacles for the diversity of tpy-based metallo-supramolecules.[11] In most of these cases, Zn(II), Cd(II) and Fe(II) only serve as the connectors in the final supramolecular structures.[12] The question this raises is whether we are able to use other metal ions to serve as connectors and to introduce potentially new functionality to the supramolecule on account of the redox properties, magnetic properties, and photo-activities of the ions.[13] Recently, Ni(II), Co(II), Mn(II), and Cu(II) were used in a self-assembly process with tpy.[14] However, this was still limited to the self-assembly of a single-type of metal ion with organic building blocks. Perhaps due to the challenges of the design and characterization of complex metal–organic building blocks, few cases have expanded the scope of this method to metal–organic ligands.[15,16]

Herein, we report the design and synthesis of four clover leaf-shaped bimetallic supramolecular structures (Scheme 1). The structures were obtained through the coordination of tetratopic metal–organic ligand **L**, which contains Ru(II), with 4 different transition metals, Zn(II), Co(II), Mn(II), and Ni(II). As

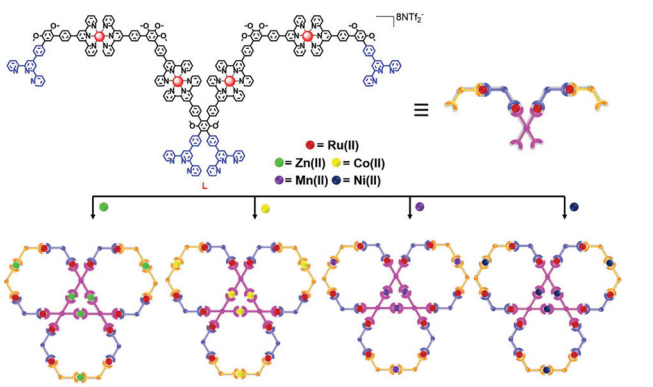


**Scheme 1** Self-assembly of clover leaf-shaped supramolecular structures obtained through the coordination of **L** with four different metal ions.

[a]*Institute of Environmental Research at Greater Bay Area; Key Laboratory for Water Quality and Conservation of the Pearl River Delta, Ministry of Education; Guangzhou Key Laboratory for Clean Energy and Materials; Guangzhou University, Guangzhou 510006, China. E-mail: chemwps@csu.edu.cn, zhezhang2018@gzhu.edu.cn*

[b]*College of Chemistry and Environmental Engineering, Shenzhen University, Shenzhen, Guangdong 518055, China. E-mail: xiaopengli@szu.edu.cn*

[c]*Guangdong Provincial Key Laboratory of Functional Supramolecular Coordination Materials and Applications, Jinan University, Guangzhou 510632, China*

†Electronic supplementary information (ESI) available: Full experimental details, the $^{1}H$ NMR, $^{13}C$ NMR, COSY, NOESY of the new compounds, ESI-MS spectra of related compounds. See DOI: 10.1039/d1qo00336d

‡These authors contributed equally to this work.

designed, these complexes exhibit distinctive redox properties. The key metal–organic ligand **L**, which has four uncomplexed terpyridinyl units, was obtained *via* a 4-fold Suzuki coupling reaction of 4-(2,2′:6′,2″-terpyridyl)-phenylboronic acid with a precursor, **5** (Scheme S1, ESI†). **L** and $Zn(NTf_2)_2$ were self-assembled in MeCN/MeOH at a stoichiometric ratio of 1 : 2. The assembly was stirred at 60 °C for 8 h followed by addition of excess $LiNTf_2$. The resulting solid was washed with water and MeOH. The reddish supramolecular metal complex $\mathbf{Zn_6L_3}$ was obtained in a relatively high yield (98%). Subsequently, self-assembly with other metals was undertaken using some common metal salts, *i.e.*, $CoCl_2{\cdot}6H_2O$, $MnClO_4{\cdot}6H_2O$ and $NiSO_4{\cdot}7H_2O$ (Scheme S2, ESI†). As a result, a series of bimetallic clover leaf-shaped supramolecules with high symmetry were obtained. The structures were characterized using 1D and 2D NMR spectroscopy, electrospray ionization-mass spectrometry (ESI-MS), traveling wave ion mobility-mass spectrometry (TWIM-MS),[17] gradient tandem-mass spectrometry ($gMS^2$),[18] transmission electron microscopy (TEM), and cyclic voltammetry (CV).

Fig. 1 shows the $^1$H NMR spectra of (a) ligand **L**, (b) $\mathbf{Zn_6L_3}$ and (c) $\mathbf{Co_6L_3}$. Three sets of distinctive signals appear at 9.11, 8.86 and 8.73 ppm, split in a 4 : 1 : 1 ratio, in the aromatic region of the spectrum of **L**. These are assigned to the three sets of $tpyH^{3',5'}$ protons of the Ru-based tpy moieties (A–D, E, and F tpy-phenyl peaks). In addition, the characteristic $tpyH^{6,6''}$ protons exhibited two sets of peaks, proving the formation of a highly symmetric structure (Fig. 1a). The other assignments were confirmed with the aid of 2D COSY and NOESY NMR spectroscopy (Fig. S16 and S17, ESI†). Shown in Fig. 1b, the signals of all the coordinated tpy moieties merged into broad peaks caused by their large planar structures. Compared with the signals of the free tpy groups of **L**, the proton signals attributed to E-$tpyH^{3',5'}$ and F-$tpyH^{3',5'}$ were shifted downfield, from 8.86 and 8.73 ppm to 9.12 ppm. Meanwhile, an expected upfield shift of the $tpyH^{6,6''}$ proton signals from 8.9 and 8.7 ppm to 7.82 ppm can be observed due to the electronic shielding effect that arises after coordination with the metals. The remaining signals of the $\mathbf{Zn_6L_3}$ spectrum were confirmed using 2D COSY and NOESY NMR spectroscopy (Fig. S20 and S21, ESI†). In order to acquire more evidence of the structure, diffusion-ordered NMR spectroscopy (DOSY) was used to measure the size of $\mathbf{Zn_6L_3}$. The DOSY spectrum (Fig. S22, ESI†) of $\mathbf{Zn_6L_3}$ shows that the protons are found in a narrow band at $\log D = -9.88$, which also demonstrates the formation of a discrete structure. The diffusion coefficient D was calculated to be $1.32 \times 10^{-10}$ m$^2$ s$^{-1}$, from which the hydrodynamic radius, according to the Stokes–Einstein equation, is 2.42 nm for $\mathbf{Zn_6L_3}$ ($D$ = 4.84 nm). This result is consistent with the modelling data (4.67 nm). The paramagnetic nature of Co(II) is well-known, therefore, the Co(II) complexes were hard to characterize using $^1$H NMR. Nevertheless, we obtained the $^1$H NMR spectrum of $\mathbf{Co_6L_3}$ (Fig. S23–25, ESI†) which spreads out over a wide range from 3 to 100 ppm (Fig. 1c). Although the 2D COSY and 2D NOESY spectra of the tpy protons could not be obtained because of fast relaxation, the $^1$H NMR signals from the tpy protons of $\mathbf{Co_6L_3}$ could be assigned based on their characteristic chemical shifts and literature reports.[14,19] Compared with Co(II), Mn(II) and Ni(II) exhibit stronger paramagnetic behaviour with shorter relaxation times, thus resulting in unsatisfactory $^1$H NMR spectra.[20]

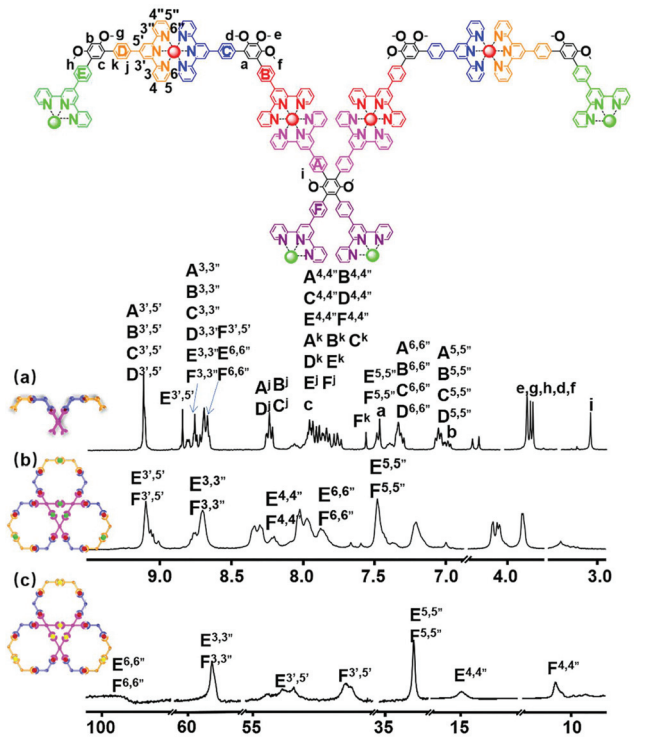


**Fig. 1** The $^1$H NMR spectra of (a) **L**, (b) $\mathbf{Zn_6L_3}$ and (c) $\mathbf{Co_6L_3}$ (500 MHz, $CDCN_3$, 300 K).

In addition, ESI-MS coupled with TWIM-MS was applied to validate the proposed structures. Fig. 2a shows a series of peaks with continuous charges from 11+ to 21+ for $\mathbf{Zn_6L_3}$ due to the successive loss of the $NTf_2^-$ counterion. After deconvolution, the obtained molecular weight of 25 007 Da agreed well with the proposed molecular composition $[(C_{234}H_{210}N_{36}O_{12})_3 Ru_{12}Zn_6(NTF_2^-)_{36}]$. The experimental isotope pattern of each charged state is consistent with the simulated isotopic distribution (Fig. S6, ESI†). TWIM-MS showed a series of charged states with a narrow drift time distribution ranging from 11+ to 20+, excluding the formation of other isomers or conformers (Fig. 2b). Moreover, the molecular weights of $\mathbf{Co_6L_3}$, $\mathbf{Mn_6L_3}$ and $\mathbf{Ni_6L_3}$ were also confirmed to correspond with their proposed molecular compositions (Fig. 2c, e and Fig. S4, ESI†). Similarly, the complexes with Co(II), Mn(II) and Ni(II) have comparable drift times in the same charge states (Fig. 2d, f and Fig. S5, ESI†), indicating that these complexes have similar shapes.

In order to examine the stability of the supramolecular complex, $gMS^2$ experiments were performed on the 17+ ions at $m/z$ 1190.4 *via* collision-induced dissociation with collision energies ranging from 4 to 28 V (Fig. 3c). There was no obvious

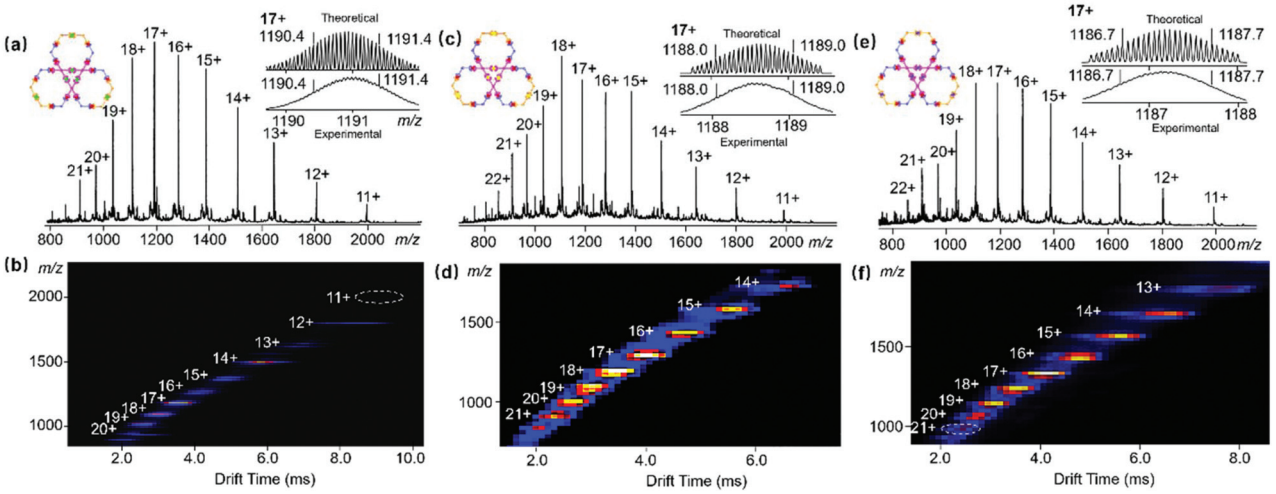


Fig. 2 ESI-MS of (a) $Zn_6L_3$, (c) $Co_6L_3$ and (e) $Mn_6L_3$; TWIM-MS plots (*m/z vs.* drift time) of (b) $Zn_6L_3$, (d) $Co_6L_3$ and (f) $Mn_6L_3$.

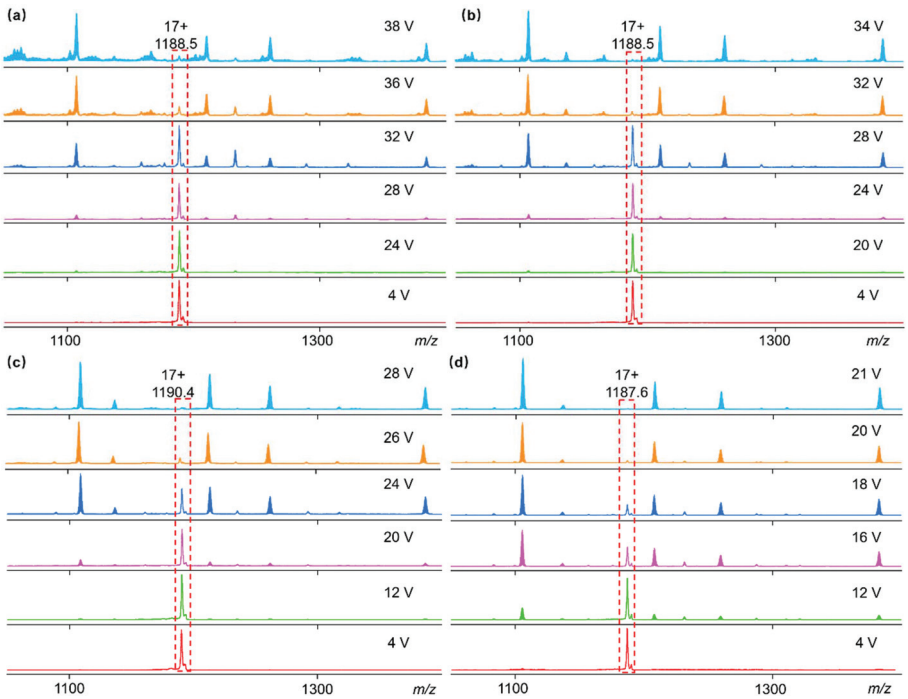


Fig. 3 $gMS^2$ of (a) $Ni_6L_3$ at *m/z* 1188.5 with different collision energies, (b) $Co_6L_3$ at *m/z* 1188.5 with different collision energies, (c) $Zn_6L_3$ at *m/z* 1190.4 with different collision energies and (d) $Mn_6L_3$ at *m/z* 1187.6 with different collision energies.

fragmentation peak observed below 20 V and when the voltage reached 28 V the complex ions completely dissociated. The stability of $Co_6L_3$, $Mn_6L_3$ and $Ni_6L_3$ was examined under the same test conditions. The 17+ ions of $Ni_6L_3$ dissociated at 38 V, while $Co_6L_3$ and $Mn_6L_3$ became fragments at 34 V and 21 V, respectively. The stabilities of these supermolecules in the gas phase were estimated and were found to depend on the metal ions with a relative order of Ni > Co > Zn > Mn. This is similar to the relative order of stabilities observed for previously reported simple complexes.[21,22]

Furthermore, TEM also provided evidence for the formation of the clover-type bimetallic supramolecular structure. As shown in Fig. 4b, a reasonable measured diameter of 4.90 nm could be observed from the TEM image. This is similar to the size simulated from molecular modelling (4.67 nm) (Fig. 4b and Fig. S26–S28, ESI†). Finally, CV was used to characterize the electrical properties of the supramolecules, and a three-electrode working system consisting of a 3 mm glassy carbon electrode (WE), platinum wire electrode (CE) and Ag/AgCl electrode (RE) was used for testing. Due to the oxidation of the

 

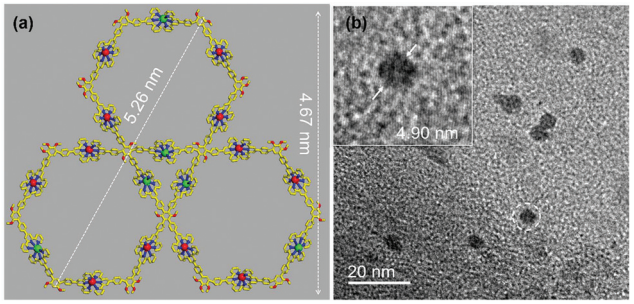


Fig. 4 (a) Representative energy-minimized structure obtained from molecular modelling of $\mathbf{Zn_6L_3}$, (b) TEM images of $\mathbf{Zn_6L_3}$.

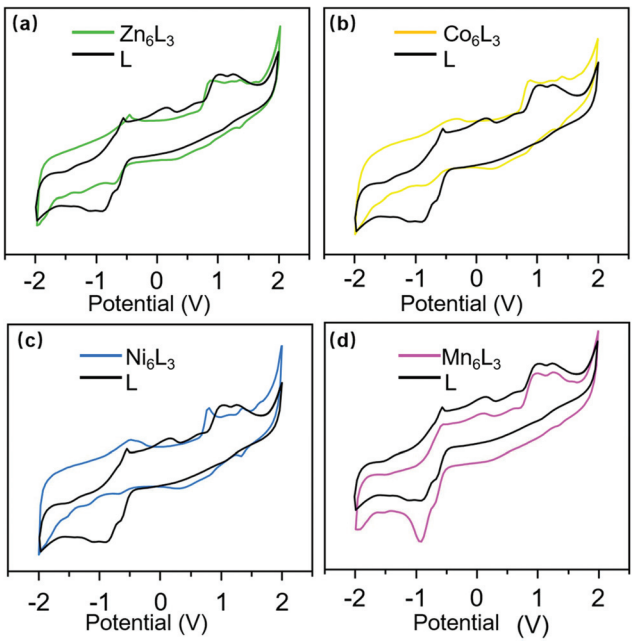


Fig. 5 CV of L with (a) $\mathbf{Zn_6L_3}$, (b) $\mathbf{Co_6L_3}$, (c) $\mathbf{Ni_6L_3}$, and (d) $\mathbf{Mn_6L_3}$ (in a 0.1 M solution of $Bu_4NPF_6$ in $CH_3CN$).

Ru(II)/Ru(III) and Ru(III)/Ru(IV) couples,[23] ligand **L** has two oxidation peaks near 1.05 and 1.25 V (Fig. 5). In contrast, the $Ru^{2+/3+}$ and $Ru^{3+/4+}$ oxidation peaks of the supramolecular structure are slightly shifted compared with ligand **L**. Since Zn(II) is already in its highest oxidation state, only the oxidation peaks of Ru can be observed at 0.84 and 1.16 V.[24] In Fig. 5b and c, the irreversible oxidation of Co(II) in $\mathbf{Co_6L_3}$ can be seen peaking at −0.35 V, while the irreversible oxidation peak of Ni(II) is located at −0.48 V. The supramolecular structure of $\mathbf{Mn_6L_3}$ gives rise to similar CV curves seen in ligand **L**.[25,26] The photochemical properties of these complexes were also studied using UV-visible spectroscopy and low temperature fluorescence spectroscopy. The absorption spectra of the ligand and all complexes have a characteristic absorption peak near 495 nm, which can be attributed to the metal-to-ligand charge transfer transitions of the tpy-Ru-tpy unit (Fig. S29, ESI†).[27] The emissions from **L** and the supramolecules were detected in $CH_3CN$ solution under 73 K (Fig. S30†). The emission spectra of $\mathbf{Ni_6L_3}$, $\mathbf{Mn_6L_3}$ and $\mathbf{Co_6L_3}$ overlapped with a major peak at 653 nm while the major peak of $\mathbf{Zn_6L_3}$ shows a slight shift to 648 nm.[28,29]

In conclusion, four clover leaf-shaped metallo-supramolecular structures were successfully designed and synthesized. This report is the first example where $Mn^{2+}$, $Co^{2+}$, $Ni^{2+}$ metal ions are used in a heterometallic multinuclear metallo-supramolecular system. The structures were characterized using 1D and 2D NMR, high-resolution ESI-MS, TWIM-MS, $gMS^2$, TEM, CV, UV-vis and fluorescence spectroscopy. Moreover, we anticipate that these multinuclear metallo-supramolecules may serve as a model system for further study of the self-assembly behavior and physical properties of 2D materials.

## Author contributions

All authors have given approval to the final version of the manuscript. Z.Z., X.L. and P.W. designed the experiments; T.W. and Q.B. completed the synthesis; T.W. and Z.T. carried out the NMR analysis; Q.B. and T.W. did the ESI-MS test and data curation; L.X., Y.G. and M.C. completed the TEM characterization; P.S. performed the low temperature fluorescence measurement; Q.B. and Z.Z. analyzed the experiment data; Q. B. and T.W. wrote the manuscript; Z.Z., X.L., H.W., T.X. and P. W. edited the manuscript. All the authors discussed the results and commented on and proofread the manuscript.

## Conflicts of interest

There are no conflicts to declare.

## Acknowledgements

This research was supported by the National Natural Science Foundation of China (21971257 to P.W., 21806027 to P.S.), the Guangdong Natural Science Foundation (2019A1515011358 to Z.Z., 2018A030313479 to P.S.), the Science and Technology Research Project of Guangzhou (202002030257 to Z.Z.), the Open Fund of Guangdong Provincial Key Laboratory of Functional Supramolecular Coordination Materials and Applications (2020A07 to Z.Z.). The authors thank Dr Bokai Liao for the CV tests and the TEM tests from the Modern Analysis and Testing Center of Guangzhou University.

## Notes and references

1 (*a*) R. Chakrabarty, P. S. Mukherjee and P. J. Stang, Supramolecular coordination: self-assembly of finite two- and three-dimensional ensembles, *Chem. Rev.*, 2011, **111**, 6810–6918; (*b*) M. D. Ward and P. R. Raithby, Functional behaviour from controlled self-assembly: challenges and prospects, *Chem. Soc. Rev.*, 2013, **42**, 1619–1636.

2 (*a*) M. Han, D. M. Engelhard and G. H. Clever, Self-assembled coordination cages based on banana-shaped ligands, *Chem. Soc. Rev.*, 2014, **43**, 1848–1860; (*b*) G. R. Newkome and C. N. Moorefield, From 1 → 3 dendritic designs to fractal supramacromolecular constructs: understanding the pathway to the Sierpiński gasket, *Chem. Soc. Rev.*, 2015, **44**, 3954–3967; (*c*) H. Wang, Y. Li, N. Li, A. Filosa and X. Li, Increasing the size and complexity of discrete 2D metallosupramolecules, *Nat. Rev. Mater.*, 2020, **6**, 145–167.

3 M. Schulze, V. Kunz, P. D. Frischmann and F. Wurthner, A supramolecular ruthenium macrocycle with high catalytic activity for water oxidation that mechanistically mimics photosystem II, *Nat. Chem.*, 2016, **8**, 576–583.

4 (*a*) L.-J. Chen, Y.-Y. Ren, N.-W. Wu, B. Sun, J.-Q. Ma, L. Zhang, H. Tan, M. Liu, X. Li and H.-B. Yang, Hierarchical self-assembly of discrete organoplatinum(II) metallacycles with polysaccharide via electrostatic interactions and their application for heparin detection, *J. Am. Chem. Soc.*, 2015, **137**, 11725–11735; (*b*) Y. Liu, L. Perez, A. D. Gill, M. Mettry, L. Li, Y. Wang, R. J. Hooley and W. Zhong, Site-selective sensing of histone methylation enzyme activity via an arrayed supramolecular tandem assay, *J. Am. Chem. Soc.*, 2017, **139**, 10964–10967.

5 Y.-R. Zheng, K. Suntharalingam, T. C. Johnstone and S. J. Lippard, Encapsulation of Pt(IV) prodrugs within a Pt(II) cage for drug delivery, *Chem. Sci.*, 2015, **6**, 1189–1193.

6 K. Schwamborn and R. M. Caprioli, Molecular imaging by mass spectrometry-looking beyond classical histology, *Nat. Rev. Cancer*, 2010, **10**, 639–646.

7 (*a*) Z.-Y. Li, Y. Zhang, C.-W. Zhang, L.-J. Chen, C. Wang, H. Tan, Y. Yu, X. Li and H.-B. Yang, Cross-linked supramolecular polymer gels constructed from discrete multi-pillar [5]arene metallacycles and their multiple stimuli-responsive behavior, *J. Am. Chem. Soc.*, 2014, **136**, 8577–8589; (*b*) H. Wang, X. Qian, K. Wang, M. Su, W.-W. Haoyang, X. Jiang, R. Brzozowski, M. Wang, X. Gao, Y. Li, B. Xu, P. Eswara, X.-Q. Hao, W. Gong, J.-L. Hou, J. Cai and X. Li, Supramolecular Kandinsky circles with high antibacterial activity, *Nat. Commun.*, 2018, **9**, 1815–1824; (*c*) X. Yan, T. R. Cook, J. B. Pollock, P. Wei, Y. Zhang, Y. Yu, F. Huang and P. J. Stang, Responsive supramolecular polymer metallogel constructed by orthogonal coordination-driven self-assembly and host/guest interactions, *J. Am. Chem. Soc.*, 2014, **136**, 4460–4463.

8 (*a*) J.-H. Fu, Y.-H. Lee, Y.-J. He and Y.-T. Chan, Facile self-assembly of metallo-supramolecular ring-in-ring and spiderweb structures using multivalent terpyridine ligands, *Angew. Chem., Int. Ed.*, 2015, **54**, 6231–6235; (*b*) T.-Z. Xie, S.-Y. Liao, K. Guo, X. Lu, X. Dong, M. Huang, C. N. Moorefield, S. Z. D. Cheng, X. Liu, C. Wesdemiotis and G. R. Newkome, Construction of a highly symmetric nanosphere via a one-pot reaction of a tristerpyridine ligand with Ru(II), *J. Am. Chem. Soc.*, 2014, **136**, 8165–8168.

9 Z. Jiang, Y. Li, M. Wang, B. Song, K. Wang, M. Sun, D. Liu, X. Li, J. Yuan, M. Chen, Y. Guo, X. Yang, T. Zhang, C. N. Moorefield, G. R. Newkome, B. Xu, X. Li and P. Wang, Self-assembly of a supramolecular hexagram and a supramolecular pentagram, *Nat. Commun.*, 2017, **8**, 15476–15485.

10 Z. Zhang, Y. Li, B. Song, Y. Zhang, X. Jiang, M. Wang, R. Tumbleson, C. Liu, P. Wang, X.-Q. Hao, T. Rojas, A. T. Ngo, J. L. Sessler, G. R. Newkome, S. W. Hla and X. Li, Intra- and intermolecular self-assembly of a 20 nm-wide supramolecular hexagonal grid, *Nat. Chem.*, 2020, **12**, 468–474.

11 T. Wu, J. Yuan, B. Song, Y.-S. Chen, M. Chen, X. Xue, Q. Liu, J. Wang, Y.-T. Chan and P. Wang, Stepwise self-assembly of a discrete molecular honeycomb using a multitopic metallo-organic ligand, *Chem. Commun.*, 2017, **53**, 6732–6735.

12 S. Chakraborty and G. R. Newkome, Terpyridine-based metallosupramolecular constructs: tailored monomers to precise 2D-motifs and 3D-metallocages, *Chem. Soc. Rev.*, 2018, **47**, 3991–4016.

13 X. Yang, D. Zhang, J. Li, W. Ji, N. Yang, S. Gu, Q. Wu, Q. Jiang, P. Shi and L. Li, A mitochondrion-targeting Mn(II)-terpyridine complex for two-photon photodynamic therapy, *Chem. Commun.*, 2020, **56**, 9032–9035.

14 L. Wang, B. Song, S. Khalife, Y. Li, L.-J. Ming, S. Bai, Y. Xu, H. Yu, M. Wang, H. Wang and X. Li, Introducing seven transition metal ions into terpyridine-based supramolecules: self-assembly and dynamic ligand exchange study, *J. Am. Chem. Soc.*, 2020, **142**, 1811–1821.

15 T.-Z. Xie, X. Wu, K. J. Endres, Z. Guo, X. Lu, J. Li, E. Manandhar, J. M. Ludlow, C. N. Moorefield, M. J. Saunders, C. Wesdemiotis and G. R. Newkome, Supercharged, precise, megametallodendrimers via a single-step, quantitative, assembly process, *J. Am. Chem. Soc.*, 2017, **139**, 15652–15655.

16 M. Chen, J. Wang, S.-C. Wang, Z. Jiang, D. Liu, Q. Liu, H. Zhao, J. Yan, Y.-T. Chan and P. Wang, Truncated Sierpiński triangular assembly from a molecular mortise-tenon joint, *J. Am. Chem. Soc.*, 2018, **140**, 12168–12174.

17 S. Perera, X. Li, M. Soler, A. Schultz, C. Wesdemiotis, C. N. Moorefield and G. R. Newkome, Hexameric palladium(II) terpyridyl metallomacrocycles: assembly with 4,4′-bipyridine and characterization by TWIM mass spectrometry, *Angew. Chem., Int. Ed.*, 2010, **49**, 6539–6544.

18 X. Li, Y.-T. Chan, G. R. Newkome and C. Wesdemiotis, Gradient tandem mass spectrometry interfaced with Ion mobility separation for the characterization of supramolecular architectures, *Anal. Chem.*, 2011, **83**, 1284–1290.

19 E. C. Constable, K. Harris, C. E. Housecroft, M. Neuburger and J. A. Zampese, Turning $\{M(tpy)_2\}^{n+}$ embraces and CH···π interactions on and off in homoleptic cobalt(II) and cobalt(III) bis(2,2′: 6′,2″-terpyridine) complexes, *CrystEngComm*, 2010, **12**, 2949–2961.

20 H. S. Chow, E. C. Constable, C. E. Housecroft, K. J. Kulicke and Y. Tao, When electron exchange is chemical exchange-assignment of $^1$H NMR spectra of paramagnetic cobalt(II)-

 

2,2′: 6′,2″-terpyridine complexes, *Dalton Trans.*, 2005, **2**, 236–237.

21 M. Satterfield and J. S. Brodbelt, Relative binding energies of gas-phase pyridyl ligand/metal complexes by energy-variable collisionally activated dissociation in a quadrupole ion trap, *Inorg. Chem.*, 2001, **40**, 5393–5400.

22 M. A. Meier, B. G. Lohmeijer and U. S. Schubert, Relative binding strength of terpyridine model complexes under matrix-assisted laser desorption/ionization mass spectrometry conditions, *J. Mass Spectrom.*, 2003, **38**, 510–516.

23 M. Chen, D. Liu, J. Huang, Y. Li, M. Wang, K. Li, J. Wang, Z. Jiang, X. Li and P. Wang, Trefoiled propeller-shaped spiral terpyridyl metal-organic architectures, *Inorg. Chem.*, 2019, **58**, 11146–11154.

24 Z. Zhang, H. Wang, X. Wang, Y. Li, B. Song, O. Bolarinwa, R. A. Reese, T. Zhang, X.-Q. Wang, J. Cai, B. Xu, M. Wang, C. Liu, H.-B. Yang and X. Li, Supersnowflakes: stepwise self-assembly and dynamic exchange of rhombus star-shaped supramolecules, *J. Am. Chem. Soc.*, 2017, **139**, 8174–8185.

25 N. Elgrishi, M. B. Chambers, V. Artero and M. Fontecave, Terpyridine complexes of first row transition metals and electrochemical reduction of $CO_2$ to CO, *Phys. Chem. Chem. Phys.*, 2014, **16**, 13635–13644.

26 I. F. Mansoor, D. I. Wozniak, Y. Wu and M. C. Lipke, A delocalized cobaltoviologen with seven reversibly accessible redox states and highly tunable electrochromic behaviour, *Chem. Commun.*, 2020, **56**, 13864–13867.

27 K. C. Robson, B. D. Koivisto, T. J. Gordon, T. Baumgartner and C. P. Berlinguette, Triphenylamine-modified ruthenium(II) terpyridine complexes: enhancement of light absorption by conjugated bridging motifs, *Inorg. Chem.*, 2010, **49**, 5335–5337.

28 X.-J. Yang, F. Drepper, B. Wu, W.-H. Sun, W. Haehnel and C. Janiak, From model compounds to protein binding: syntheses, characterizations and fluorescence studies of $[RuII(bipy)(terpy)L]^{2+}$ complexes (bipy = 2,2′-bipyridine; terpy = 2,2′: 6′,2″-terpyridine; L = imidazole, pyrazole and derivatives, cytochrome c), *Dalton Trans.*, 2005, **2**, 256–267.

29 M. Galletta, S. Campagna, M. Quesada, G. Ulrich and R. Ziessel, The elusive phosphorescence of pyrromethene-$BF_2$ dyes revealed in new multicomponent species containing Ru(II)-terpyridine subunits, *Chem. Commun.*, 2005, **33**, 4222–4224.